Journal of Computational Mathematics, Vol.19, No.5, 2001, 475–488.

SYMPLECTIC SCHEMES FOR QUASILINEAR WAVE EQUATIONS OF KLEIN-GORDON AND SINE-GORDON TYPE*

Xiao-wu Lu

(*Department of Mathematics and Computer Science, Emory University, Atlanta, GA 30322, USA*)

Abstract

A class of finite difference methods of first- and second-order accuracy for the computation of solutions to the quasilinear wave equations is presented. These difference methods are constructed based on the symplectic schemes to the infinite-dimensional Hamiltonian system. Numerical experiments are presented to demonstrate the superior performance of these methods.

Key words: Symplectic integration, Sine-Gordon equations, Finite difference method.

1. Introduction

There has been much discussion recently about designing symplectic numerical schemes for both finite and infinite dimensional Hamiltonian systems ([1] - [8]). A class of symplectic schemes for linear wave equations has been suggested [1], and numerical experiments for these schemes have been conducted [8, 9]. Results show that the symplectic methods are inherently free from artificial dissipation and all kinds of non-Hamiltonian pollutions, and are thus of high quality and resolution.

In this paper, we try to generalize the discussion in the previous studies [1, 4, 5, 8], and construct symplectic schemes for one-dimensional quasilinear wave equation [11]

$$\partial_t^2 u - \partial_x f(\partial_x u) + g(u) = 0 \tag{1}$$

where g is a smooth function with $g(0) = 0$, $f^{'}(u) \geq \delta > 0$ and $uf^{''}(u) > 0$ for $u \neq 0$. Equation (1) models a vibrating string with an elastic external positional force, and has many applications in the study of nonlinear wave phenomena. Equations such as the Klein-Gordon, Sine-Gordon and the Φ^4 system may be all categorized within the system (1). The aim of this paper is to design numerical methods with high quality and resolution that can be used in the numerical computation of solutions for system (1). Since (1) can be written as an infinite-dimensional Hamiltonian system, it is our belief that the numerical methods that are constructed based upon the symplectic schemes will perform much better than other conventional methods, and thus will be good candidates for numerical simulation and calculation. The numerical methods we present here are constructed based on the similar procedures suggested in [1], and may be regarded as a generalized version of the schemes for the linear wave equation.

The paper is organized as follows: In section 2, we give a brief overview of general symplectic schemes and generating functional. In section 3, we construct a class of first- and second-order

* Received April 2, 1997; Final revised August 19, 1999.

accurate difference methods for the quasilinear wave equations that result from the general schemes. The numerical results for these methods are presented in section 4, followed by conclusions in section 5.

2. Symplectic Schemes and Generating Functional

Symplectic schemes for both finite- and infinite-dimensional Hamiltonian systems have been widely discussed in the literature ([1]–[8]). In this section, we give a brief review of these schemes for infinite-dimensional Hamiltonian systems. Interested readers may consult the literature [1, 4, 6, 7] for details.

We consider $\mathcal{M}$ be a vector subspace of $C^\infty(R)\times C^\infty(R)$ consisting of those (u,v) with both $\mid u(x)\mid$ and $\mid v(x)\mid$ decreasing sufficiently rapidly such that the integral we write below is valid, and define $\mathcal{F}(\mathcal{M})=\{F(u,v)\mid F:$ real-valued functional on $\mathcal{M}\}$. The symplectic structure on $\mathcal{M}$ is

$$\omega((u_1,v_1),(u_2,v_2))=\int_{-\infty}^{\infty}(u_1,v_1)J\,(u_2,v_2)^T\;dx. \tag{2}$$

where $J=\begin{pmatrix}0&-1\\1&0\end{pmatrix}$. An infinite-dimensional Hamiltonian system on $\mathcal{M}$ takes the form

$$\partial_t u=-\frac{\delta H}{\delta v}(u,v,t),\qquad \partial_t v=\frac{\delta H}{\delta u}(u,v,t), \tag{3}$$

where $u=u(x,t), v=v(x,t)$ are two real functions, and $u(x,t), v(x,t)\in\mathcal{M}$ for any fixed t. $H(u,v)\in\mathcal{F}(\mathcal{M})$ is an energy functional in Hamiltonian mechanics. Within the Hamiltonian framework, the solution (u,v) of system (3) can be regarded as a Hamiltonian flow on the space $\mathcal{M}$ generated by a time-dependent map g^t, i.e., $(u(x),v(x))(t)=g^t\cdot(u_0,v_0)$, where $(u_0,v_0)=(u_0(x),v_0(x))\in\mathcal{M}$ is an initial condition. Furthermore, the map $g^t:\mathcal{M}\to\mathcal{M}$ is symplectic [10].

Since g^t is a symplectic map, it is naturally required that any numerical approximation to the system (3) should be carried out in such way that the discretized $(\Delta t,\Delta x)$-map should still be symplectic after the time and spatial discretization.

In this section, we will show how to construct a symplectic integrator (in the time direction) for system (3). First we will introduce a 4×4 Darboux matrix.

Definition [Darboux matrix]. *A 4×4 matrix T is called a Darboux if*

$$T^*\begin{pmatrix}0&-I\\I&0\end{pmatrix}T=\begin{pmatrix}J&0\\0&-J\end{pmatrix}, \tag{4}$$

where I is a 2×2 identity matrix, and $J=\begin{pmatrix}0&-1\\1&0\end{pmatrix}$.

In this paper, however, we will narrow down the class of Darboux matrices to a subclass of normal Darboux matrices, i.e., those which satisfy the conditions of $A+B=0$, $C+D=I$. Then the normal Darboux matrices can be characterized as

$$T=\begin{pmatrix}A&B\\C&D\end{pmatrix}=\begin{pmatrix}J&-J\\\frac{1}{2}(I+JL)&\frac{1}{2}(I-JL)\end{pmatrix} \tag{5}$$

and its inverse

$$T^{-1} = \begin{pmatrix} A_1 & B_1 \\ C_1 & D_1 \end{pmatrix} = \begin{pmatrix} \frac{1}{2}(JLJ - J) & I \\ \frac{1}{2}(JLJ + J) & I \end{pmatrix}, \tag{6}$$

where L is a 2×2 real symmetric matrix.

For each Hamiltonian functional H with a normal Darboux matrix, a generating functional Φ can be defined. This generating functional satisfies the Hamilton-Jacobi equation

$$\frac{d\Phi(W,t)}{dt} = -H(A_1 \nabla \Phi(W) + B_1 W) \tag{7}$$

and can be expressed by the Taylor series in t:

$$\Phi(W,t) = \sum_{k=1}^{\infty} \phi^{(k)}(W) t^k, \qquad |\, t \,| \;\; small. \tag{8}$$

The coefficients $\phi^{(k)}(W)$ in (8) can be determined recursively

$$\phi^{(1)}(W) = -H(W), \tag{9}$$

and for $k = 2, 3, \cdots$,

$$\phi^{(k)} = \frac{-1}{k} \sum_{m=1}^{k-1} \frac{1}{m!} \sum_{i_1, \cdots, i_m = 1}^{2} H_{i_1, \cdots, i_m}(W) \sum_{j_1 + \cdots + j_m = k-1, j_l \geq 1} (A_1 \nabla \phi^{(j_1)})_{i_1} \cdots (A_1 \nabla \phi^{(j_m)})_{i_m}, \tag{10}$$

where $W \in \mathcal{M}$, A_1 is the upper-left sub-block of T^{-1}, and the notation $(\quad)_{i_1}$ denotes the i_1-th component of a vector.

The generating functional is closely related to the symplectic scheme. Consider equation (3) is solved on a discrete time mesh $\{n\Delta t, n = 0, 1, \cdots\}$, where Δt is the time step. We denote $u^n = u(x, n\Delta t)$ and $v^n = (x, n\Delta t)$; then, based on the generating functional, a symplectic scheme of m-th order accuracy for system (3) can be written as

$$\bar{W}^{n+1} = \sum_{k=1}^{m} \nabla \phi^{(k)}(W^n) \Delta t, \tag{11}$$

where the function $\phi^{(k)}, k = 1, 2, \cdots, m$ is defined as in (9) and (10), and two vectors $\bar{W}^{n+1} \in \mathcal{M}$, $W^n \in \mathcal{M}$ are defined as

$$\bar{W}^{n+1} = \begin{pmatrix} \bar{w_1}^{n+1} \\ \bar{w_2}^{n+1} \end{pmatrix} = A \begin{pmatrix} u^{n+1} \\ v^{n+1} \end{pmatrix} + B \begin{pmatrix} u^n \\ v^n \end{pmatrix}, \tag{12}$$

$$W^n = \begin{pmatrix} w_1^n \\ w_2^n \end{pmatrix} = C \begin{pmatrix} u^{n+1} \\ v^{n+1} \end{pmatrix} + D \begin{pmatrix} u^n \\ v^n \end{pmatrix}. \tag{13}$$

3. Numerical Schemes for Quasilinear Wave Equations

In this section, we construct symplectic methods for quasilinear wave equation (1) based on the symplectic scheme (11) discussed in the previous section.

Generally speaking, a numerical integration of a time-dependent PDE may often be conceived as consisting of two parts: spatial discretization and time discretization. During both spatial and time discretizations, the spatial (or time) derivatives are approximated by finite differences, finite elements, spectral methods, etc. However, for a Hamiltonian PDE, since its Hamiltonian flow is symplectic, it is required that the time (or spatial) discretization preserve the symplectic property.

The approach we take to construct symplectic schemes for equation (1) is pretty straightforward. It consists of the following two steps: In step 1, we discretize (1) in the time direction first, and reduce it to a semi-discretized ODE system with unknowns (u^n, v^n) defined on the discrete time mesh $\{n\Delta t, n = 0, 1, \cdots\}$. During the time discretization step, the configuration space $\mathcal{M}$ remains unchanged, and the symplectic structure ω on $\mathcal{M}$ is preserved. In step 2, we approximate the spatial derivatives using values of the functions (u^n, v^n) defined on the spatial grids $\{j\Delta x, j = 1, \cdots N\}$, which is denoted as $\bar{\mathcal{M}} = \{z = (u_1^n, \cdots, u_N^n, v_1^n, \cdots, v_N^n) | n = 1, \cdots\} (\approx R^{2N})$. During the spatial discretization step, the configuration space is reduced from $\mathcal{M}$ to $\bar{\mathcal{M}}$, and the corresponding symplectic structure $\bar{\omega}$ on $\bar{\mathcal{M}}$:

$$\bar{\omega}(z_1, z_2) = z_1 \; J \; z_2^T, \tag{14}$$

is preserved (Figure 1).

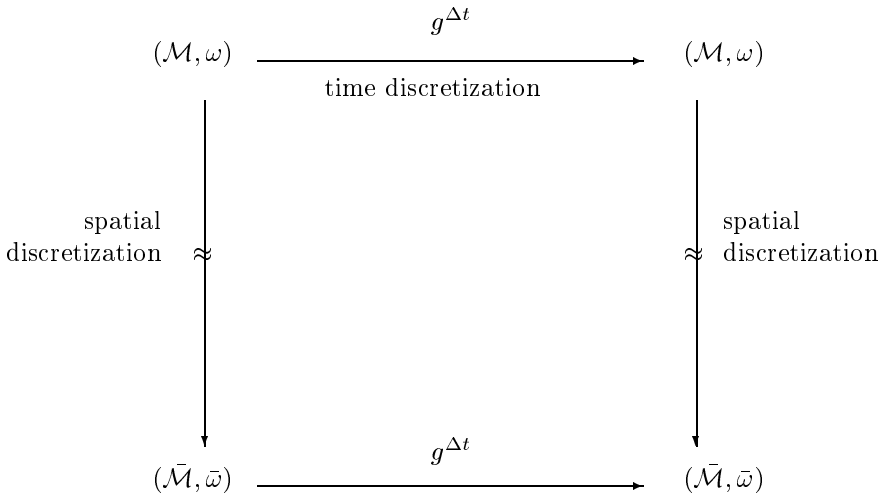

Figure 1: Time and spatial discretization steps during the construction of symplectic schemes for equation (1).

3.1. Discretization in Time Direction

We use the symplectic scheme discussed in the previous section to perform time discretization for system (1).

By letting $v = -\partial_t u$, equation (1) can be easily put into the Hamiltonian formulation (3) with Hamiltonian functional $H = \int_R (v^2/2 + F(u_x) + G(u))dx$ and $F' = f$, $G' = g$.

The normal Darboux given in the previous section is only in general form. One can specify a normal Darboux based on the selection of real symmetric matrix L during the construction of the scheme. Here, we will select one of the simplest forms of matrix L, $L = \begin{pmatrix} 0 & 1 \\ 1 & 0 \end{pmatrix}$. Therefore, the matrix T has the following form

$$T = \begin{pmatrix} 0 & -1 & 0 & 1 \\ 1 & 0 & -1 & 0 \\ 0 & 0 & 1 & 0 \\ 0 & 1 & 0 & 0 \end{pmatrix}. \tag{15}$$

Based on this selection of T, we can compute $\bar{W}^{n+1}$ and W^n as

$$\bar{W}^{n+1} = \begin{pmatrix} v^n - v^{n+1} \\ u^{n+1} - u^n \end{pmatrix}, \quad W^n = \begin{pmatrix} u^n \\ v^{n+1} \end{pmatrix}. \tag{16}$$

The first two terms of generating function Φ in (9)-(10) can be computed explicitly

$$\phi^{(1)}(W^n) = \phi^{(1)}(u^n, v^{n+1}) = -H(u^n, v^{n+1}) \tag{17}$$

$$\phi^{(2)}(W^n) = \phi^{(2)}(u^n, v^{n+1}) = \frac{1}{2} v^{n+1}(g(u^n) - \partial_x f(u_x^n)). \tag{18}$$

Substituting (16), (17) and (18) back into (11), we derive the following schemes

(I) semi-discretized scheme of $O(\Delta t)$ order of accuracy

$$\begin{cases} u^{n+1} &= u^n - \Delta t v^{n+1} \\ v^{n+1} &= v^n - \Delta t \partial_x f(u_x^n) + \Delta t g(u^n). \end{cases} \tag{19}$$

(II) semi-discretized scheme of $O(\Delta t^2)$ order of accuracy

$$\begin{cases} u^{n+1} = u^n - \Delta t v^{n+1} + \frac{\Delta t^2}{2}(g(u^n) - \partial_x f(u_x^n)) \\ v^{n+1} = v^n + \Delta t(g(u^n) - \partial_x f(u_x^n)) + \frac{\Delta t^2}{2}[\partial_x(v_x^{n+1} f'(u_x^n)) - v^{n+1} g'(u^n)]. \end{cases} \tag{20}$$

3.2. Discretization in space direction

After time discretization, the semi-discretized systems (19) and (20) are symplectic. In order to be used in the practical computation, both schemes need to be further discretized in the spatial direction.

The spatial discretization is basically a dimensional reduction process, during which the the infinite-dimensional space $\mathcal{M}$, on which the semi-discretized systems are defined, is reduced to a finite-dimensional space $\bar{\mathcal{M}}$. For symplectic approach, it is natural to require that the spatial discretization should also maintain the symplectic structure $\bar{\omega}$ on $\bar{\mathcal{M}}$.

The way of selecting spatial discretization is crucial for remaining the symplectic property. In this paper, we will use the central difference to replace $\partial_x f(u_x^n)$ in (19) and (20) with

$$\partial_x f(u_x^n) \approx \frac{1}{\Delta x}(\bar{f}_{j+\frac{1}{2}} - \bar{f}_{j-\frac{1}{2}}), \tag{21}$$

where

$$\bar{f}_{j+\frac{1}{2}} = f((u_x^n)_{j+\frac{1}{2}}) = f(\frac{u_{j+1}^n - u_j^n}{\Delta x}). \tag{22}$$

Once applying the central approximation (21) for spatial derivatives in both schemes (19) and (20), we get a scheme of $O(\Delta t) + O(\Delta x^2)$ order of accuracy

$$\left\{ \begin{array}{lcl} u_j^{n+1} & = & u_j^n - \Delta t v_j^{n+1} \\ v_j^{n+1} & = & v_j^n - \frac{\Delta t}{\Delta x}(\bar{f}_{j+\frac{1}{2}} - \bar{f}_{j-\frac{1}{2}}) + \Delta t g(u_j^n) \end{array} \right. \tag{23}$$

and a scheme of $O(\Delta t^2) + O(\Delta x^2)$ order of accuracy

$$\left\{ \begin{array}{l} u_j^{n+1} = u_j^n - \Delta t v_j^{n+1} - \frac{\Delta t^2}{2\Delta x}(\bar{f}_{j+\frac{1}{2}} - \bar{f}_{j-\frac{1}{2}}) + \frac{\Delta t^2}{2} g(u_j^n) \\ (1 + \frac{\Delta t^2}{2} g^{'}(u_j^n)) v_j^{n+1} = v_j^n + \Delta t g(u_j^n) - \frac{\Delta t}{\Delta x}(\bar{f}_{j+\frac{1}{2}} - \bar{f}_{j-\frac{1}{2}}) \\ \qquad\qquad + \frac{\Delta t^2}{2\Delta x}[\bar{v}_{j+\frac{1}{2}}^{n+1} \bar{f}^{'}_{j+\frac{1}{2}} - \bar{v}_{j-\frac{1}{2}}^{n+1} \bar{f}^{'}_{j-\frac{1}{2}}], \end{array} \right. \tag{24}$$

where $\bar{v}_{j+\frac{1}{2}}^{n+1} = \frac{v_{j+1}^{n+1} - v_j^{n+1}}{\Delta x}$, $\bar{v}_{j-\frac{1}{2}}^{n+1} = \frac{v_j^{n+1} - v_{j-1}^{n+1}}{\Delta x}$ and $\bar{f}^{'}_{j+\frac{1}{2}} = f^{'}(\frac{u_{j+1}^n - u_j^n}{\Delta x})$.

The central difference we choose here is important in order to remain the symplectic structure during the space variable discretization. In fact, we can prove the following the following Theorem:

Theorem 1. *Scheme (23) preserves symplectic structure $\bar{\omega}$ on the phase space $\bar{\mathcal{M}}$.*

Proof. Let $u^n = (u_1^n, \cdots, u_N^n), v^n = (v_1^n, \cdots, v_N^n)$, we denote each element in $\bar{\mathcal{M}}$ as (u^n, v^n). The scheme (23) can be rewritten as

$$\begin{array}{rcl} (u^{n+1}, v^{n+1}) & = & \bar{g}^{\Delta t}(u^n, v^n) \\ & = & \left(\begin{array}{cc} I & -\Delta t\, I \\ 0 & I \end{array} \right) \left(\begin{array}{c} u^n \\ v^n - \frac{\Delta t}{\Delta x} \vec{f}(u^n) + \vec{g}(u^n) \end{array} \right), \end{array} \tag{25}$$

where $\vec{f}(u^n)$ and $\vec{g}(u^n)$ are vector functions with $N-$component which are defined as

$$\vec{f}(u^n) = F(u_1, \cdots, u_N) = (\bar{f}_{1+\frac{1}{2}}, \bar{f}_{2+\frac{1}{2}} - \bar{f}_{2-\frac{1}{2}}, \cdots, -\bar{f}_{N-\frac{1}{2}})^T \tag{26}$$

$$\vec{g}(u^n) = (g(u_1^n),\, g(u_2^n),\, \cdots,\, g(u_N^n))^T. \tag{27}$$

In order to show scheme (23) preserves symplectic structure, we only need to verify $\bar{g}^{\Delta t}$ is symplectic, i.e.,

$$\left[\frac{\partial \bar{g}^{\Delta t}(u^n, v^n)}{\partial (u^n, v^n)} \right]^T J \;\; \frac{\partial \bar{g}^{\Delta t}(u^n, v^n)}{\partial (u^n, v^n)} = J \tag{28}$$

Notice that

$$\frac{\partial \bar{g}^{\Delta t}(u^n, v^n)}{\partial (u^n, v^n)} = \left(\begin{array}{cc} I & -\Delta t\, I \\ 0 & I \end{array} \right) \left(\begin{array}{cc} I & 0 \\ -B & I \end{array} \right) = \left(\begin{array}{cc} I + \Delta t\, B & -\Delta t\, I \\ -B & I \end{array} \right), \tag{29}$$

where $B = (b_{ij})$ is a symmetric tridiagonal matrix

$$b_{ij} = \left\{ \begin{array}{ll} g^{'}(u_j^n) - \frac{\Delta t}{\Delta x^2}[\bar{f}^{'}_{i+\frac{1}{2}} + \bar{f}^{'}_{i-\frac{1}{2}}], & \text{for } i = j; \\ -\frac{\Delta t}{\Delta x^2} \bar{f}^{'}_{i-\frac{1}{2}}, & \text{for } j = i-1; \\ -\frac{\Delta t}{\Delta x^2} \bar{f}^{'}_{i+\frac{1}{2}}, & \text{for } j = i+1; \\ 0, & \text{elsewise.} \end{array} \right. \tag{30}$$

Thus,

$$\begin{aligned}
&\left[\frac{\partial \bar{g}^{\Delta t}(u^n, v^n)}{\partial (u^n, v^n)}\right]^T J \frac{\partial \bar{g}^{\Delta t}(u^n, v^n)}{\partial (u^n, v^n)} \\
&\quad = \begin{pmatrix} I + \Delta t\, B & -\Delta t\, I \\ -B & I \end{pmatrix}^T \begin{pmatrix} 0 & -I \\ I & 0 \end{pmatrix} \begin{pmatrix} I + \Delta t\, B & -\Delta t\, I \\ -B & I \end{pmatrix} \\
&\quad = \begin{pmatrix} (I + \Delta t\, B)\, B - B(I + \Delta t\, B) & -(I + \Delta t\, B) + \Delta t\, B \\ -\Delta t\, B + I + \Delta t\, B & \Delta t\, I - \Delta t\, I \end{pmatrix} \\
&= \begin{pmatrix} 0 & -I \\ I & 0 \end{pmatrix} = J. \qquad (31)
\end{aligned}$$

Similarly, we can prove the following theorem:

Theorem 2. *Scheme (24) preserves symplectic structure $\bar{\omega}$ on the phase space $\bar{\mathcal{M}}$.*

4. Numerical Results

Several test problems have been designed to test the effectiveness of the above schemes (23) and (24), and the numerical results are presented. We use both schemes (23) and (24) to compute the numerical solution of each test problem. Also, we calculate and present both the maximum and the L^2-norm of numerical errors for solution u, which are defined as

$$\|e^n\|_{max} = \max_i |u_i^n - u(n\Delta t, i\Delta x)| \qquad (32)$$

$$\|e^n\|_{L^2} = (\sum_i |u_i^n - u(n\Delta t, i\Delta x)|^2 \Delta x)^{1/2} \qquad (33)$$

where u_i^n and $u(n\Delta t, i\Delta x)$ are numerical and analytic solutions defined on the space-time grids $\{(i\Delta x, n\Delta t) \mid i = 0, 1 \cdots, N, n = 0, 1, 2, \cdots\}$, respectively.

4.1. Klein-Gordon Equation

We consider the initial-boundary value problem of (1) on the domain $[0, 1] \times (0, \infty)$, with $f(\partial_x u) = \partial_x u / a^2$ and $g(u) = -(1 + \pi^2)u$, where the parameter a is an integer. The initial and boundary conditions are set to

$$u(x, 0) = \sin(a\pi x), \qquad u_t(x, 0) = \sin(a\pi x), \qquad (34)$$

$$u(0, t) = 0, \qquad u(1, t) = 0. \qquad (35)$$

The equation possesses the analytic solution

$$u(x, t) = \exp(t) \sin(a\pi x). \qquad (36)$$

We use schemes (23) and (24) to solve equation (1) with initial and boundary conditions (34) and (35) for different values of parameter a. The spatial step is selected as $\Delta x = 0.01$ through all the computations. A sample of values of the resulting numerical errors at $t = 1.5$, corresponding to the parameter values $a = 1.0, a = 3.0$ and $a = 8.0$ is given in Table 1. Several snapshots of the

numerical solution at $t = 0.6, 1.0$ and 1.7 for different values of parameter a are shown in Figure 1. The analytic solutions are also plotted in the same pictures for comparison. These results show quite clearly that the schemes generate numerical solutions with very good accuracy, even for rapidly oscillating solutions like $\sin(a\pi x)$ with $a = 8.0$.

Table 1. The numerical errors for the Klein-Gordon equation given by schemes (23) and (24) at $t = 1.5$, corresponding to the different values of a and time step Δt, while the space step $\Delta x = 0.01$ is fixed.

a	Iteration Number (Δt)	Scheme (23)		Scheme (24)	
		$\|e\|_{max}$	$\|e\|_{L^2}$	$\|e\|_{max}$	$\|e\|_{L^2}$
1.0	150 (0.01)	1.2467D-2	8.8154D-3	2.0890D-3	1.4772D-3
	300 (0.005)	7.1791D-3	5.0761D-3	1.9213D-3	1.3581D-3
	600 (0.0025)	4.5251D-3	3.1991D-3	1.9213D-3	1.3581D-3
3.0	75 (0.02)	3.8068D-2	2.6918D-2	1.7703D-2	1.2518D-2
	150 (0.01)	2.7486D-2	1.9435D-2	1.7019D-2	1.2034D-2
	300 (0.005)	2.2135D-2	1.5664D-2	1.6848D-2	1.1914D-2
	600 (0.0025)	1.9476D-2	1.3771D-2	1.6806D-2	1.1883D-2
8.0	75 (0.02)	1.4223D-1	1.0077D-1	1.2073D-1	8.5534D-2
	150 (0.01)	1.3104D-1	9.2843D-2	1.1998D-1	8.5007D-2
	300 (0.005)	1.2540D-1	8.8847D-2	1.1980D-1	8.4875D-2
	600 (0.0025)	1.2257D-1	8.6842D-2	1.1972D-1	8.4842D-2

4.2. Sine-Gordon Type Equation

We consider two Sine-Gordon-type equations: Sine-Gordon equation with $f(u) = u$, $g(u) = \sin u$ in (1), and Φ^4 equation with $f(u) = u$, $g(u) = -u + u^3$ in (1), respectively.

Both equations have "kink" or "anti-kink" solitary wave solutions. For the Sine-Gordon equation, its "kink" solution is $u(x,t) = 4\arctan(\exp\frac{(x-\nu t)}{\sqrt{(1-\nu^2)}})$, which corresponds with the initial condition

$$u(x,0) = 4\arctan(e^{\frac{x}{\sqrt{1-\nu^2}}}), u_t(x,0) = \frac{-2\nu}{\sqrt{1-\nu^2}}\operatorname{sech}(e^{\frac{x}{\sqrt{1-\nu^2}}}). \tag{37}$$

Similarly, for the Φ^4 equation, direct integration establishes the existence of an "anti-kink"

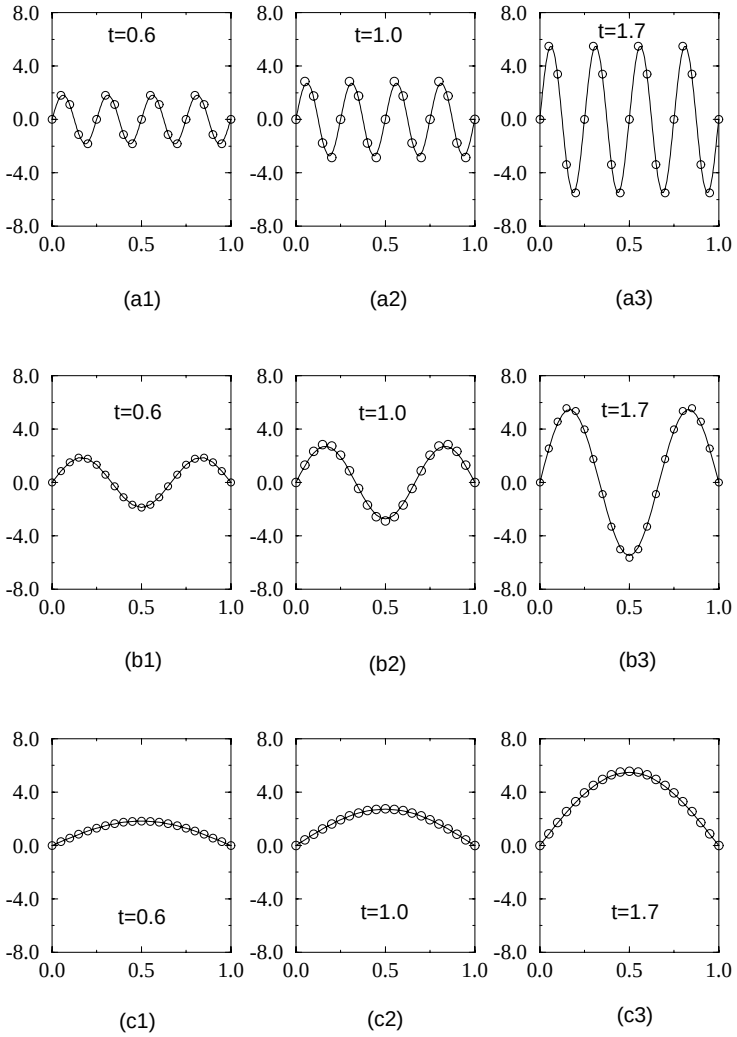

Figure 2: Numerical solution of the Klein-Gordon equation given by scheme (23) at $t = 0.6$, 1.0 and $t = 1.7$, corresponding to different values of parameter a. (a1–a3), $a = 8.0$; (b1–b3), $a = 3.0$; (c1–c3), $a = 1.0$.

type solitary wave $u(x,t) = \tanh\left((-x+\nu t)/\sqrt{2(1-\nu^2)}\right)$, which corresponds with the initial condition

$$u(x,0) = \tanh\left(\frac{-x}{\sqrt{2(1-\nu^2)}}\right), u_t(x,0) = \frac{\nu}{\sqrt{2(1-\nu^2)}}\operatorname{sech}^2\left(\frac{-x}{\sqrt{2(1-\nu^2)}}\right) \tag{38}$$

where ν is a constant.

Both problems are solved numerically using scheme (23) and (24). We calculated the motion of the single "kink" solution for the Sine-Gordon equation and the "anti-kink" solution for the

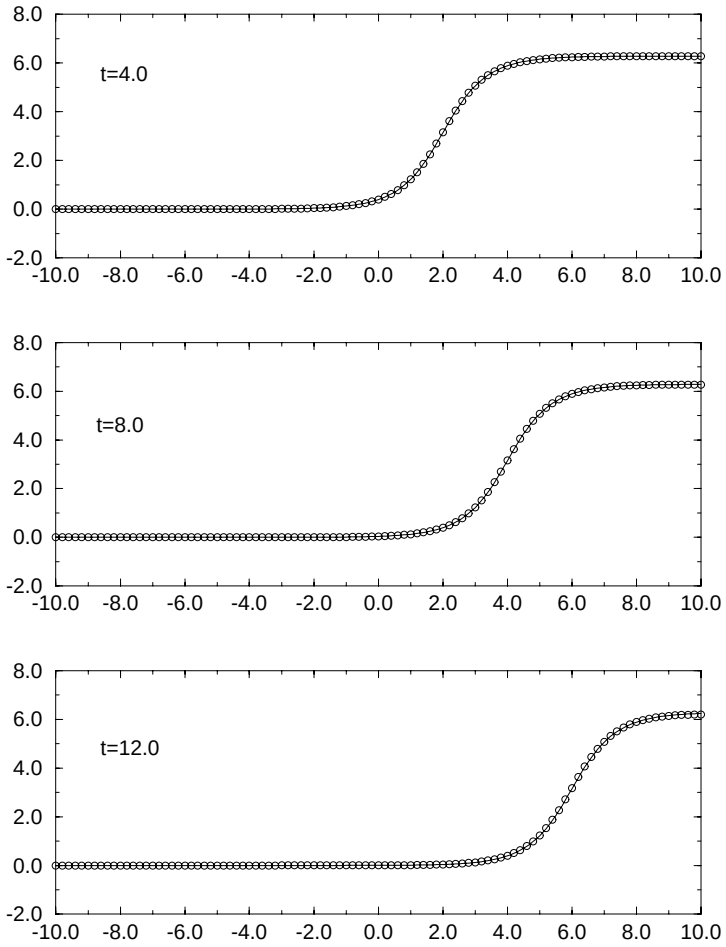

Figure 3: Numerical solution of the Sine-Gordon equation given by scheme (23) at $t = 4.0$, 8.0 and 12.0. The solid line represents the analytic solution, while the circle represents the numerical solution.

Φ^4 equation with $\nu = 12$. All the numerical calculations were performed on the spatial grids that range from $[-10, 10]$, with the spatial step Δx is set to 0.2. Tables 2 and 3 contain a selection of values of resulting numerical errors at $t = 12.0$ for the Sine-Gordon and the Φ^4 equation, respectively. Figures 3 and 4 present plots of kink and anti-kink solutions at times $t = 4.0, 8.0$ and 12.0 for the Sine-Gordon and the Φ^4 equation, respectively. Again, the analytic solutions are also plotted in the same picture for comparison. The results indicate that the numerical solutions perfectly predict the actual position of the "kink" or "anti-kink" solitary waves, and essentially have no oscillation.

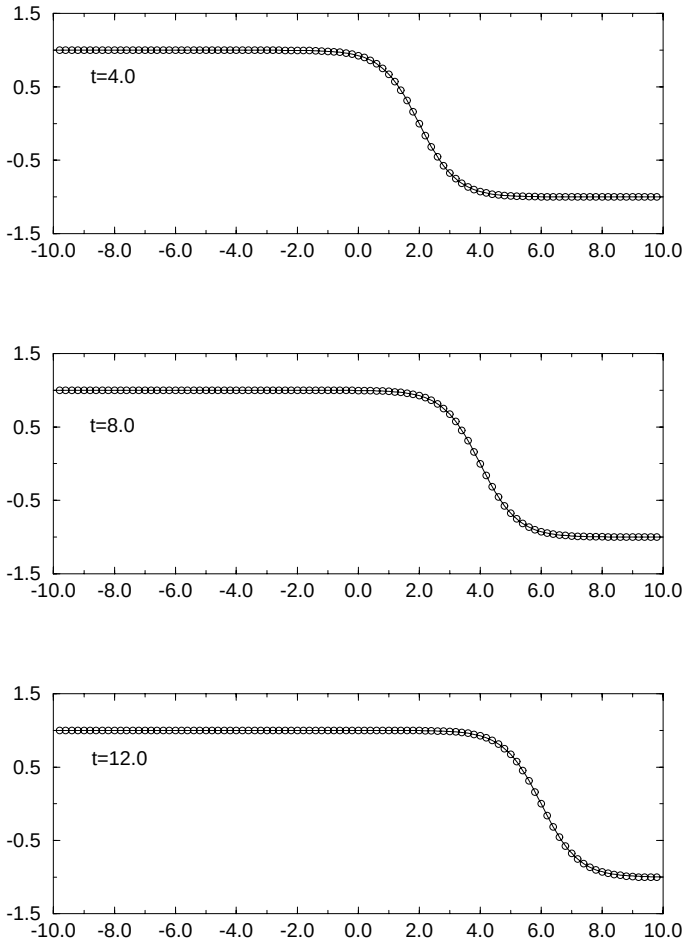

Figure 4: Numerical solution of the Φ^4 equation given by scheme (23) at $t = 4.0$, 8.0 and 12.0. The solid line represents the analytic solution, while the circle represents the numerical solution.

Table 2. The numerical errors for the Sine-Gordon equation give by schemes (23) and (24) at $t = 12.0$. The space step $\Delta x = 0.2$ is fixed.

Iteration Step	Scheme (23)		Scheme (24)	
(Δt)	$\|e\|_{max}$	$\|e\|_{L^2}$	$\|e\|_{max}$	$\|e\|_{L^2}$
120 (0.1)	4.2951D-2	4.3881D-2	5.1844D-2	7.0452D-2
240 (0.05)	4.0908D-2	4.6239D-2	3.6496D-2	5.2697D-2
600 (0.02)	3.9686D-2	4.7785D-2	3.6932D-2	4.8869D-2
1200 (0.01)	3.9276D-2	4.8288D-2	3.6884D-2	4.8591D-2
2400 (0.005)	3.9071D-2	4.8534D-2	3.6370D-2	4.8627D-2

Table 3. The errors of numerical solution for the Φ^4 equation give by schemes (23) and (24) at $t = 12.0$. The space step $\Delta x = 0.2$ is fixed.

Iteration Step	Scheme (23)		Scheme (24)	
(Δt)	$\|e\|_{max}$	$\|e\|_{L^2}$	$\|e\|_{max}$	$\|e\|_{L^2}$
120 (0.1)	9.5750D-3	1.4263D-2	2.1621D-2	2.7642D-2
240 (0.05)	1.1692D-2	1.5654D-2	1.5326D-2	1.9471D-2
600 (0.02)	1.2711D-2	1.6383D-2	1.3612D-2	1.7231D-2
1200 (0.01)	1.3009D-2	1.6602D-2	1.3368D-2	1.6912D-2
2400 (0.005)	1.3151D-2	1.6706D-2	1.3307D-2	1.6833D-2

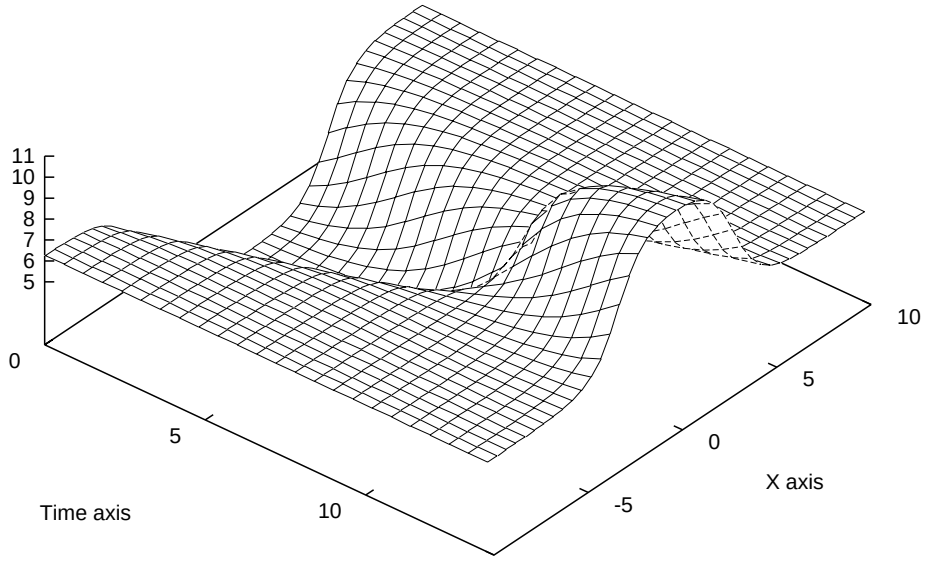

Figure 5: Simulation results of kink and anti-kink solitary waves collision in the Sine-Gordon equation give by scheme (24).

Next, we use these schemes to simulate the collision process of two solitary waves in both Sine-Gordon and Φ^4 equations. It is well known that in the Sine-Gordon equation, two solitary waves will pass through each other without any intervention (with only a phase shift); however,

it is not possible for these solitary waves to pass through each other in the Φ^4 equation. The resulting state is more complicated and largely dependent on parameter ν [13, 14]. Again, our numerical schemes reproduce these phenomena very well. In our numerical calculation, a kink with $v = -0.5$ and an anti-kink with $v = 0.5$ are initially placed at the positions $x = 5.0$ and $x = -5.0$, respectively. The calculation domain is $[-10, 10]$ with the time step $\Delta t = 0.05$ and the spatial step $\Delta x = 0.5$. The entire collision process is presented in a space-time plot. Figure 5 illustrates the kink and anti-kink collision in the Sine-Gordon equation. As time develops, the two solitary waves approach each other, interact nonlinearly, and then emerge unchanged in shape. Figure 6 shows the collision of two solitary waves in the Φ^4 equation, where those two waves bounce backward after colliding.

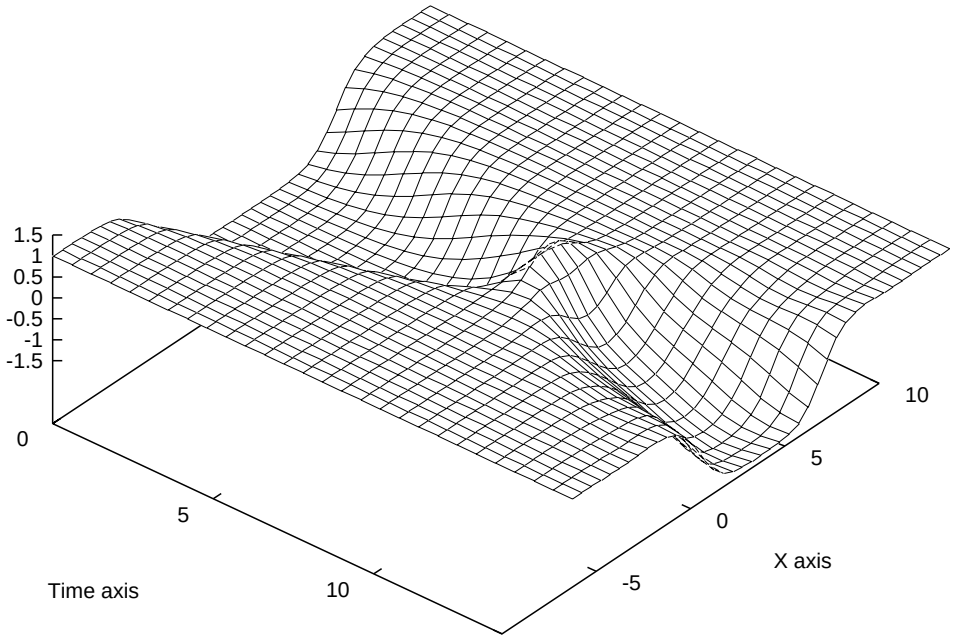

Figure 6: Simulation results of kink and anti-kink solitary waves collision in the Φ^4 equation given by scheme (24).

5. Conclusion

We present a class of difference methods of first- and second-order accuracy for the quasilinear wave equations based on the symplectic schemes. Numerical experiments for these methods

are also carried out on the Klein-Gordon and the Sine-Gordon equations. Our results show that such methods excel over the conventional methods, with favorable properties such as high resolution, low oscillation, and low dissipation. The long-term tracking capability for these methods is remarkable. The results also suggest that the methods can be used as effective tools for the numerical study of the solutions of the quasilinear wave equations.

References

[1] C. Li, M. Qin, A symplectic difference scheme for the infinite dimensional Hamilton system, *J. Comput. Math.*, **6**:2 (1988), 164-174.

[2] K. Feng, Difference schemes for Hamiltonian formalism and symplectic geometry, *J. Comput. Math.*, **4**:3 (1986), 279-289.

[3] K. Feng, M. Qin, The symplectic methods for the computation of Hamiltonian equation, Proc. of 1st Chinese Conf. on Numerical Methods of PDE's, Lecture Notes in Mathematics, 1297, Ed. Zhu You-lan and Guo Ben-Yu, Springer-Verlag, (1987), 1-37.

[4] K. Feng, H. Wu, M. Qin, D. Wang, Construction of Canonical difference schemes for Hamiltonian formalism via generating functions, *J. Comput. Math.*, **7**:1 (1989), 71-96.

[5] M. Qin, M. Zang, Multi-stage symplectic schemes of two kinds of Hamiltonian systems for wave equations, *Comp. Math. Appl.*, **19** (1990), 51-62.

[6] K. Feng, M. Qin, Hamiltonian algorithms and a comparative numerical study, *Computer Physics Communication*, **65** (1991), 173-187.

[7] M. Qin, D. Wang, M. Zhang, Explicit symplectic difference scheme for separatable Hamiltonian system, *J. Comput. Math.*, **9**:3 (1991), 211-221.

[8] X. Lu, R. Schmid, A symplectic algorithm for wave equations, *Mathematics and Computers in Simulation*, **43**:1 (1997), 29-38.

[9] X. Lu and R. Schmid, A difference method to wave equation based on symplectic integration, *Proceedings of the 14th IMACS World Congress*, Atlanta, GA, June 1994.

[10] P. Chernoff, J. Marsden, Properties of Infinite Dimensional Hamilton System, Lecture Notes in Mathematics, 425, Springer, New York.

[11] P. Marcati, R. Natalini, Global weak entropy solutions to quasilinear wave equations of Klein-Gordon and Sine-Gordon Type, *IEEE Trans. Comput.*, **38**:11 (1989), 1526-1538.

[12] R.D. Richtmyer, Difference Methods for Initial-Value Problems, Intersciences, New York, 1961.

[13] D.K. Campbell, J.F. Schonfeld and C. A. Wingate, Resonance windows in kink-antikink interactions in Φ^4 theory, *Physica D*, **9** (1983), 1-32.

[14] D.K. Campbell, M. Peyrard, P. Sodano, Kink-antikink interactions in the double Sine-Gordon equation, *Physica D*, **19** (1986), 165-205.